An Algebraic Treatment of Essential Boundary Conditions in the Particle–Partition of Unity Method

Marc Alexander Schweitzer

Institut für Numerische Simulation, Universität Bonn, Wegelerstr. 6, D-53115 Bonn, Germany
schweitzer@ins.uni-bonn.de

Summary. This paper is concerned with the treatment of essential boundary conditions in meshfree methods. In particular we focus on the particle–partition of unity method (PPUM). However, the proposed technique is applicable to any partition of unnity based approach.

We present an efficient scheme for the automatic construction of a direct splitting of a PPUM function space into the degrees of freedom suitable for the approximation of the Dirichlet data and the degrees of freedom that remain for the approximation of the PDE by simple linear algebra. Notably, our approach requires no restrictions on the distribution of the discretization points nor on the employed (local) approximation spaces.

We attain the splitting of the global function space from the respective direct splittings of the employed local approximation spaces. Hence, the global splitting can be computed with (sub-)linear complexity. Due to this direct splitting of the meshfree PPUM function space we can implement a conforming local treatment of essential boundary data so that the realization of Dirichlet boundary values in the meshfree PPUM is straightforward. The presented approach yields an optimally convergent scheme which is demonstrated by the presented numerical results.

Key words: meshfree method, partition of unity method, essential boundary conditions, Nitsche's method

1 Introduction

The implementation of essential boundary conditions in meshfree methods (MM) is in general not trivial which is one of the drawbacks of MM. This is due to the fact that the meshfree shape functions in general do not satisfy essential boundary conditions explicitly; i.e., the shape functions do not satisfy the Kronecker condition. Many different techniques have been suggested to overcome this issue, see e.g. [1,12,14,15,17,19–23,26] and the references within.

A very general and probably the most promising approach (up to now) is the application of Nitsche's method [25] in the meshfree context [1, 17, 21]. Even though this non-conforming approach yields an optimally convergent meshfree scheme it suffers from some drawbacks.

Nitsche's method is based on a specific analytical modification of the weak formulation of the considered partial differential equation (PDE). This modification employs all available boundary information to construct a symmetric positive definite bilinear form for a particular discretization space V. Hence, the bilinear form in Nitsche's method changes if we change the configuration of the boundary values or the discretization space V. This however might require the analytical derivation of a new appropriate bilinear form by hand. Furthermore, the bilinear form arising from Nitsche's method employs a regularization parameter which must be estimated every time we change the configuration of the boundary values or the discretization space. These issues render the user-driven interactive changing of boundary conditions unfeasible with Nitsche's method.

In this paper we present a very efficient and fully automatic scheme which allows for the conforming treatment of essential boundary conditions in meshfree methods based on simple linear algebra only. The presented algebraic approach overcomes the aforementioned drawbacks of Nitsche's approach completely and allows for an interactive changing of boundary conditions in meshfree methods. The proposed approach is applicable to all partition of unity (PU) based meshfree (or mesh-based) methods. In essence, we construct a direct splitting

$$V = V_K \oplus V_I$$

of the discretization space V (which does not satisfy the boundary conditions) separating the degrees of freedom for the approximation of the boundary conditions from the degrees of freedom used to approximate the PDE and collect them in the sub-spaces $V_I \subset H_0^k(\Omega)$ and $V_K \subset H_D^k(\Omega)$ respectively. That is the (classical) bilinear form is definite on V_I and the trace operator on the Dirichlet boundary is definite on V_K. In principle such a splitting can be constructed for any arbitrary function space and hence any numerical method. However, such a construction can in general not be computed with linear complexity and is therefore prohibitively expensive. In a partition of unity method (PUM) though we can construct an appropriate splitting of the global approximation space V^{PU} by local operations only, i.e., in (sub-)linear complexity. This is due to the specific structure of the function space

$$V^{\mathrm{PU}} := \sum_{i=1}^{N} \varphi_i V_i$$

where $\{\varphi_i\}$ denotes a PU with respect to the computational domain Ω and V_i are local approximation spaces defined on $\mathrm{supp}(\varphi_i)$ respectively. Thus, a *valid* global splitting of V^{PU} can be obtained from appropriate local splittings of the spaces V_i, i.e.

$$\sum_{i=1}^{N} \varphi_i V_i = V^{\mathrm{PU}} = V_K^{\mathrm{PU}} \oplus V_I^{\mathrm{PU}} := \sum_{i=1}^{N} \varphi_i V_{i,K} \oplus \sum_{i=1}^{N} \varphi_i V_{i,I}.$$

Note however that we ensure the global definiteness of the bilinear form on V_K^{PU} only by the use of a flat-top partition of unity [18]. The global trace operator must not be definite with respect to the global basis of V_I^{PU}. It is sufficient to obtain the definiteness of the local trace operators with respect to $V_{i,I}$ for all $i = 1, \ldots, N$. Note further that we impose no a priori constraints on the distribution of the discretization points nor on the employed local approximation spaces V_i.

The remainder of this paper is organized as follows. In Section 2 we shortly review the particle–partition of unity method [14, 27] (PPUM) and introduce the notion of a flat-top PU. The implementation of essential boundary conditions in the PPUM is subject of Section 3. Here, we shortly review Nitsche's method and derive our conforming algebraic treatment of essential boundary conditions which yields optimal convergence properties. The results of our numerical experiments are presented in Section 4. Here, we consider the approximation of regular and singular solutions and compare the quality of our new scheme with that of Nitsche's method. This comparison clearly shows that we obtain an optimally convergent conforming scheme and its overall accuracy is comparable to that of Nitsche's method. Finally, we conclude with some remarks in Section 5.

2 Particle–Partition of Unity Method

In this section let us shortly review the core ingredients of the PPUM, see [15, 16, 27] for details. In a first step, we need to construct a PPUM space V^{PU}, i.e., we need to specify the PPUM functions $u^{\mathrm{PU}} \in V^{\mathrm{PU}}$. An arbitrary function $u^{\mathrm{PU}} \in V^{\mathrm{PU}}$ is defined as the linear combination

$$u^{\mathrm{PU}}(x) = \sum_{i=1}^{N} \varphi_i(x) u_i(x) \quad \text{with} \quad u_i(x) = \sum_{m=1}^{d_i} u_i^m \vartheta_i^m(x) \tag{2.1}$$

and the respective PPUM space V^{PU} is defined as

$$V^{\mathrm{PU}} := \sum_{i=1}^{N} \varphi_i V_i \quad \text{with} \quad V_i := \mathrm{span}\langle \vartheta_i^m \rangle. \tag{2.2}$$

Here, we assume that the functions φ_i form a partition of unity (PU) on the domain Ω and refer to the spaces V_i with $\dim(V_i) = d_i$ as local approximation spaces. Hence, the shape functions employed in the PPUM are the products $\varphi_i \vartheta_i^n$ of a PU function φ_i and a local basis function ϑ_i^n. With these shape functions, we then set up a sparse linear system of equations $A\tilde{u} = \hat{f}$ via the

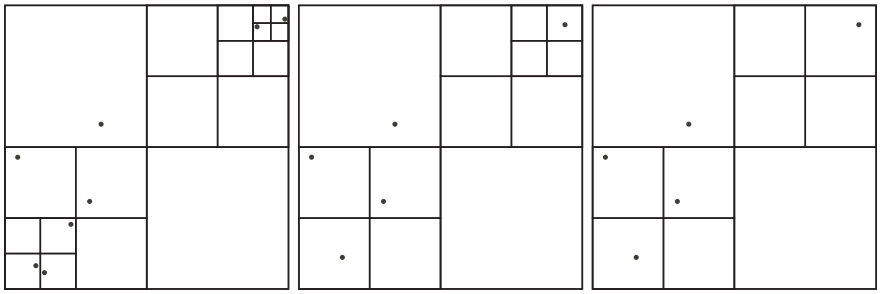

Fig. 1. Subdivision corresponding to a cover on level $J = 4$ with initial point cloud (left), derived coarser subdivisions on level 3 (center), and level 2 (right) with respective coarser point cloud.

classical Galerkin method. The linear system is then solved by our multilevel iterative solver [16, 18].

Let us now specify the particular choices for the PU functions φ_i and local approximation space V_i employed in our PPUM. The fundamental construction principle employed in [15] for the construction of the PU $\{\varphi_i\}$ is a d-binary tree. Based on the given point data $P = \{x_i \,|\, i = 1, \ldots, N\}$, we sub-divide a bounding-box $\mathcal{C}_\Omega \supset \Omega$ of the domain Ω until each cell

$$\mathcal{C}_i = \prod_{l=1}^{d} (c_i^l - h_i^l, c_i^l + h_i^l)$$

associated with a leaf of the tree contains at most a single point $x_i \in P$, see Figure 1. We obtain an overlapping cover $C_\Omega := \{\omega_i\}$ from this tree by defining the cover patches ω_i by simple uniform and isotropic scaling

$$\omega_i := \prod_{l=1}^{d} (c_i^l - \alpha h_i^l, c_i^l + \alpha h_i^l), \quad \text{with } \alpha > 1. \tag{2.3}$$

Note that we define a cover patch ω_i for leaf-cells $\mathcal{C}_i$ that contain a point $x_i \in P$ as well as for *empty* cells that do not contain any point from P. The coarser covers C_Ω^k are defined considering coarser versions of the constructed tree, i.e., by removing a complete set of leaves of the tree, see Figure 1. For details of this construction see [15, 16, 27].

To obtain a PU on a cover C_Ω^k with $N_k := \mathrm{card}(C_\Omega^k)$ we define a weight function $W_{i,k} : \Omega \to \mathbb{R}$ with $\mathrm{supp}(W_{i,k}) = \omega_{i,k}$ for each cover patch $\omega_{i,k}$ by

$$W_{i,k}(x) = \begin{cases} \mathcal{W} \circ T_{i,k}(x) & x \in \omega_{i,k} \\ 0 & \text{else} \end{cases} \tag{2.4}$$

with the affine transforms $T_{i,k} : \overline{\omega}_{i,k} \to [-1, 1]^d$ and $\mathcal{W} : [-1, 1]^d \to \mathbb{R}$ the reference d-linear B-spline. By simple averaging of these weight functions we obtain the functions

$$\varphi_{i,k}(x) := \frac{W_{i,k}(x)}{S_{i,k}(x)}, \quad \text{with} \quad S_{i,k}(x) := \sum_{l=1}^{N_k} W_{l,k}(x). \tag{2.5}$$

We refer to the collection $\{\varphi_{i,k}\}$ with $i = 1, \ldots, N_k$ as a partition of unity since there hold the relations

$$\begin{aligned} &0 \;\leq\; \varphi_{i,k}(x) \leq 1, && \sum_{i=1}^{N_k} \varphi_{i,k} \equiv 1 \text{ on } \overline{\Omega}, \\ &\|\varphi_{i,k}\|_{L^\infty(\mathbb{R}^d)} \leq C_{\infty,k}, && \|\nabla \varphi_{i,k}\|_{L^\infty(\mathbb{R}^d)} \leq \frac{C_{\nabla,k}}{\operatorname{diam}(\omega_{i,k})} \end{aligned} \tag{2.6}$$

with constants $0 < C_{\infty,k} < 1$ and $C_{\nabla,k} > 0$ so that the assumptions of the error analysis given in [3] are satisfied by our PPUM construction. Furthermore, the PU (2.5) based on the cover $C_\Omega^k = \{\omega_{i,k}\}$ obtained from the scaling of a tree decomposition (2.3) satisfies the flat-top property (for a particular choice of $\alpha > 1$), see [18,28] (and compare Figure 2).

Definition 1 (Flat-top property). *Let $\{\varphi_i\}$ be a partition of unity satisfying (2.6). Let us define the sub-patches $\omega_{\mathrm{FT,i}} \subset \omega_i$ such that $\varphi_i|_{\omega_{\mathrm{FT,i}}} \equiv 1$. Then, the PU is said to have the flat top property, if there exists a constant C_{FT} such that for all patches ω_i*

$$\mu(\omega_i) \leq C_{\mathrm{FT}}\, \mu(\omega_{\mathrm{FT,i}}) \tag{2.7}$$

where $\mu(A)$ denotes the Lebesgue measure of $A \subset \mathbb{R}^d$. We have $C_\infty = 1$ for a PU with the flat top property.

This property is essential to ensure that the product functions $\varphi_{i,k}\vartheta_{i,k}^n$ are linearly independent, provided that the employed local approximation functions $\vartheta_{i,k}^n$ are linearly independent with respect to $\omega_{\mathrm{FT,i}} = \{x \in \omega_{i,k} \,|\, \varphi_{i,k}(x) = 1\}$. Hence, we obtain global stability of the product functions $\varphi_{i,k}\vartheta_{i,k}^n$ from the local stability of the approximation functions $\vartheta_{i,k}^n$.

In general the local approximation space $V_{i,k} := \operatorname{span}\langle \vartheta_{i,k}^n \rangle$ associated with a particular patch $\omega_{i,k}$ of a PPUM space V_k^{PU} consists of two parts: A smooth approximation space, e.g. polynomials $\mathcal{P}^{p_{i,k}}(\omega_{i,k}) := \operatorname{span}\langle \psi_i^s \rangle$, and an enrichment part $\mathcal{E}_{i,k}(\omega_{i,k}) := \operatorname{span}\langle \eta_i^t \rangle$, i.e.

$$V_{i,k}(\omega_{i,k}) = \mathcal{P}^{p_{i,k}}(\omega_{i,k}) \oplus \mathcal{E}_{i,k}(\omega_{i,k}) = \operatorname{span}\langle \psi_i^s, \eta_i^t \rangle.$$

Note that we assume that the collection of functions $\langle \psi_i^s, \eta_{i,k}^t \rangle$ provide a stable basis for the space $V_{i,k}(\omega_{i,k})$ i.e. that $V_{i,k} = \mathcal{P}^{p_{i,k}} \oplus \mathcal{E}_{i,k}$ can be written as a direct sum. For most enrichment approaches [5,6,9–11,24] this is in general not the case. However for the PPUM we can always provide such a direct splitting independent of the employed enrichment spaces $\mathcal{E}_{i,k}$ [29,30].

With the help of the shape functions $\varphi_{i,k}\vartheta_{i,k}^n$ we then discretize a PDE in weak form

$$a(u,v) = \langle f, v \rangle$$

via the classical Galerkin method to obtain a discrete linear system of equations $A\tilde{u} = \hat{f}$. Note that the PU functions (2.5) in the PPUM are in general piecewise rational functions only. Therefore, the use of an appropriate numerical integration scheme [16] is indispensable in the PPUM as in most meshfree approaches [2, 4, 7, 8]. Moreover, the functions $\varphi_{i,k}\vartheta^n_{i,k}$ in general do not satisfy the Kronecker property. Thus, the coefficients $\tilde{u}_k := (u^n_{i,k})$ of a discrete function

$$u^{\mathrm{PU}}_k = \sum_{i=1}^{N_k} \varphi_{i,k} \sum_{n=1}^{d_{i,k}} u^n_{i,k}\vartheta^n_{i,k} = \sum_{i=1}^{N_k} \varphi_{i,k} \Big(\sum_{s=1}^{d^{\mathcal{P}}_{i,k}} u^s_{i,k}\psi^s_{i,k} + \sum_{t=1}^{d^{\mathcal{E}}_{i,k}} u^{t+d^{\mathcal{P}}_{i,k}}_{i,k}\eta^t_{i,k} \Big) \tag{2.8}$$

with $d^{\mathcal{P}}_{i,k} := \dim \mathcal{P}_{i,k}$, $d^{\mathcal{E}}_{i,k} := \dim \mathcal{E}_{i,k}$, and $d_{i,k} := \dim V_{i,k} = d^{\mathcal{P}}_{i,k} + d^{\mathcal{E}}_{i,k}$ on level k do not directly correspond to function values and a trivial interpolation of essential boundary data is not available.

3 Essential Boundary Conditions

The treatment of essential boundary conditions in meshfree methods is not straightforward and a number of different approaches have been suggested [1,12,14,15,17,19–23,26]. In [17] we have presented how Nitsche's method [25] can be applied successfully in the meshfree context. Here, we give a short summary of this approach. To this end, let us consider the model problem

$$\begin{aligned} \mathcal{L}(u) &:= -\mathbf{div}\,\boldsymbol{\sigma}(u) = f && \text{in } \Omega \subset \mathbb{R}^d, \\ \mathcal{B}_N(u) &:= \boldsymbol{\sigma}(u)\cdot n = g_N && \text{on } \Gamma_N \subset \partial\Omega, \\ \mathcal{B}_{D,t}(u) &:= (\boldsymbol{\sigma}(u)\cdot n)\cdot t = 0 && \text{on } \Gamma_D = \partial\Omega \setminus \Gamma_N, \\ \mathcal{B}_{D,n}(u) &:= u\cdot n = g_{D,n} && \text{on } \Gamma_D = \partial\Omega \setminus \Gamma_N. \end{aligned} \tag{3.1}$$

In the following we drop the level subscript $k = 0, \ldots, J$ for the ease of notation and define the functional

$$J_\beta(w) := \int_\Omega \boldsymbol{\sigma}(w) : \boldsymbol{\epsilon}(w)\; dx - 2\int_{\Gamma_D} ((n\cdot\boldsymbol{\sigma}(w)n)n\cdot w + \beta(w\cdot n)^2)\; ds \tag{3.2}$$

with some regularization parameter $\beta > 0$. Minimizing J_β with respect to the error $u - u^{\mathrm{PU}}$ yields the weak formulation

$$a_\beta(w,v) = l_\beta(v) \quad \text{for all } v \in V^{\mathrm{PU}} \tag{3.3}$$

with the bilinear form

$$\begin{aligned} a_\beta(u,v) := \int_\Omega \boldsymbol{\sigma}(u) : \boldsymbol{\epsilon}(v)\; dx - \int_{\Gamma_D} (n\cdot\boldsymbol{\sigma}(u)n)n\cdot v\; ds \\ - \int_{\Gamma_D} (n\cdot\boldsymbol{\sigma}(v)n)n\cdot u\; ds + \beta\int_{\Gamma_D} (u\cdot n)(v\cdot n)\; ds \end{aligned} \tag{3.4}$$

and the corresponding linear form

$$\langle l_\beta, v\rangle := \int_\Omega fv \; dx + \int_{\Gamma_N} g_N v \; ds - \int_{\Gamma_D} g_{D,n}(n \cdot \boldsymbol{\sigma}(v)n) \; ds + \beta \int_{\Gamma_D} g_{D,n} v \cdot n \; ds.$$

There is a unique solution u^{PU} of (3.3) if the regularization parameter β is chosen large enough; i.e., the regularization parameter $\beta = \beta_{V^{\mathrm{PU}}}$ is dependent on the discretization space V^{PU}. This solution u^{PU} satisfies optimal error bounds if the space V^{PU} admits the inverse estimate

$$\|(n \cdot \boldsymbol{\sigma}(v)n)\|^2_{L^2(\Gamma_D)} \;\leq\; C^2_{V^{\mathrm{PU}}} \|v\|^2_E \;=\; C^2_{V^{\mathrm{PU}}} \int_\Omega \boldsymbol{\sigma}(v) : \boldsymbol{\epsilon}(v) \; dx \tag{3.5}$$

for all $v \in V^{\mathrm{PU}}$ with a constant $C_{V^{\mathrm{PU}}}$ depending on the cover C_Ω and the employed local bases $\langle \vartheta_i^m \rangle$ only. If $C_{V^{\mathrm{PU}}}$ is known, the regularization parameter $\beta_{V^{\mathrm{PU}}}$ can be chosen as $\beta_{V^{\mathrm{PU}}} > 2C^2_{V^{\mathrm{PU}}}$ to obtain a symmetric positive definite linear system [25]. Hence, the main task associated with the use of Nitsche's approach in the PPUM context is the efficient and automatic computation of the constant $C_{V^{\mathrm{PU}}}$. To this end, we consider the inverse assumption (3.5) as a generalized eigenvalue problem and solve for the largest eigenvalue to obtain an approximation of $C^2_{V^{\mathrm{PU}}}$, see [17, 18, 27].

In summary, the PPUM discretization of our model problem (3.1) via Nitsche's approach using the space V^{PU} on the cover C_Ω is carried out in two steps: First, we estimate the regularization parameter $\beta_{V^{\mathrm{PU}}}$ from (3.5). Then, we define the weak form (3.3) and use Galerkin's method to set up the respective symmetric positive definite linear system $A\tilde{u} = \hat{f}$. This linear system is then solved by our multilevel iterative solver [16, 18].

Even though Nitsche's approach is of optimal complexity and provides an optimally convergent numerical scheme there are some drawbacks. First and foremost, there is the need to construct the appropriate functional (3.2) and the respective weak formulation (3.3) *analytically*. Since the functional depends strongly on the configuration of the boundary conditions it is not trivial to change boundary conditions in an interactive user-driven manner. Often a change in the boundary conditions requires some amount of implementation work and a re-assembly of the stiffness matrix on the boundary. Secondly, the essential boundary data is only weakly approximated and the error on the boundary is balanced with the error in the interior by Nitsche's approach. This can be inappropriate in situations where the boundary conditions need to be enforced strictly.

Let us focus on the latter issue first. The essential boundary conditions can of course be enforced (more) strictly in Nitsche's approach by increasing the regularization parameter β. In the limit $\beta \to \infty$ the essential boundary data are strictly enforced in $L^2(\Gamma_D)$ and the convergence of the scheme is still of optimal order. However the constant, i.e. the absolute value of the error, can increase. Moreover a large regularization parameter β has an severely adverse effect on the condition number of the resulting stiffness matrix rendering the solution of the linear system rather challenging.

Nevertheless let us consider the limit case $\beta \to \infty$ in some more detail. For the ease of notation let us introduce the following short-hand notation

$$\begin{aligned} V_\Omega &:= \{v \in V^{\mathrm{PU}} \mid \mathrm{supp}(v) \cap \Gamma_D = \emptyset\}, \\ V_{D,n,K} &:= \{v \in V^{\mathrm{PU}} \mid \mathrm{supp}(v) \cap \Gamma_D \neq \emptyset \text{ and } \mathcal{B}_{D,n}(v) = (v \cdot n)|_{\Gamma_d} = 0\}, \\ V_{D,n,I} &:= \{v \in V^{\mathrm{PU}} \mid \mathrm{supp}(v) \cap \Gamma_D \neq \emptyset \text{ and } \mathcal{B}_{D,n}(v) = (v \cdot n)|_{\Gamma_d} \neq 0\}. \end{aligned}$$

With $\beta \to \infty$ the bilinear form (3.4) becomes

$$a_\infty(u,v) = \begin{cases} \displaystyle\int_\Omega \boldsymbol{\sigma}(u) : \boldsymbol{\epsilon}(v)\ dx & v \in V_\Omega, \\ \displaystyle\int_\Omega \boldsymbol{\sigma}(u) : \boldsymbol{\epsilon}(v)\ dx - \int_{\Gamma_D} (n \cdot \boldsymbol{\sigma}(u)n)n \cdot v\ ds & v \in V_{D,n,K}, \\ \displaystyle\int_{\Gamma_D} (u \cdot n)(v \cdot n)\ ds & v \in V_{D,n,I}, \end{cases} \tag{3.6}$$

and we attain the respective linear form

$$\langle l_\infty, v\rangle = \begin{cases} \displaystyle\int_\Omega fv\ dx + \int_{\Gamma_N} g_N v\ ds & v \in V_\Omega, \\ \displaystyle\int_\Omega fv\ dx + \int_{\Gamma_N} g_N v\ ds - \int_{\Gamma_D} g_{D,n}(n \cdot \boldsymbol{\sigma}(v)n)\ ds & v \in V_{D,n,K}, \\ \displaystyle\int_{\Gamma_D} g_{D,n}(v \cdot n)\ ds & v \in V_{D,n,I}. \end{cases} \tag{3.7}$$

Obviously, in the case $v \in V_{D,n,K}$ we can simplify the weak form back to the classical weak formulation since $\mathcal{B}_{D,n}(u) = g_{D,n}$ and we obtain

$$\int_\Omega \boldsymbol{\sigma}(u) : \boldsymbol{\epsilon}(v)\ dx = \int_\Omega fv\ dx + \int_{\Gamma_N} g_N v\ ds \tag{3.8}$$

for all $v \in V_\Omega + V_{D,n,K}$ which involves no information about the Dirichlet boundary Γ_D. On the other hand, for $v \in V_{D,n,I}$ we need to consider the weak formulation

$$\int_{\Gamma_D} (u \cdot n)v \cdot n)\ ds = \int_{\Gamma_D} g_{D,n}(v \cdot n)\ ds \tag{3.9}$$

which involves no information about the interior Ω° or the Neumann boundary Γ_N. Note that the above consideration involves only a splitting of the test functions v only, not the trial functions u. Hence, we obtain the non-symmetric stiffness matrix A and the respective load vector $\hat{f}$ in block-form

$$A = \begin{pmatrix} A_{K,K} & A_{K,I} \\ 0 & B_{I,I} \end{pmatrix}, \qquad \hat{f} = \begin{pmatrix} \hat{f}_K \\ \hat{g}_I \end{pmatrix}. \tag{3.10}$$

where $A_{\cdot,\cdot}$ denotes the use of (3.8) and $B_{\cdot,\cdot}$ denotes the use of (3.9). Hence, the associated linear system $A\tilde{u} = \hat{f}$ can be solved by block-elimination

$$\tilde{u}_I = B_{I,I}^{-1}\hat{g}_I, \quad \tilde{u}_K = A_{K,K}^{-1}(\hat{f}_K - A_{K,I}\tilde{u}_I). \tag{3.11}$$

This is a standard technique in FEM since the kernel of the trace operator $\mathcal{B}_{D,n}$ (applied to the FEM space) is known a priori so that the above partitioning can be obtained easily. In meshfree methods as the PPUM however the kernel (applied to the meshfree function space) is *not* known a priori. Furthermore, the computation of the kernel of $\mathcal{B}_{D,n}$ is in general a *global* operation and hence prohibitively expensive. Yet, for the PPUM we can compute the (essential) kernel of the *global* operator $\mathcal{B}_{D,n}$ by *local* operations only. To be more precise we can compute a sub-space $V_I^{\mathrm{PU}} \subset V^{\mathrm{PU}}$ and a localized approximation $\hat{B}_{I,I}$ to the trace operator $\mathcal{B}_{D,n}$ that is invertible on $V_I^{\mathrm{PU}} \subset V^{\mathrm{PU}}$.

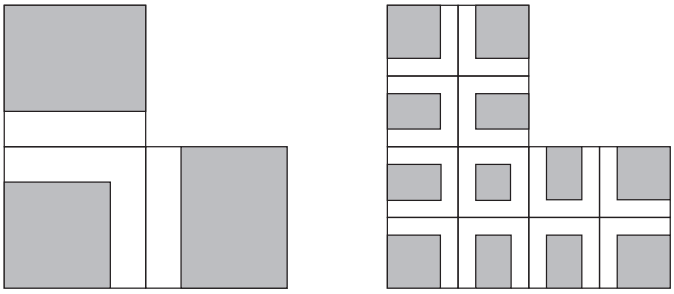

Fig. 2. Schematic of the tree decomposition of an L-shaped domain Ω on level $k = 1$ (left) and level $k = 2$ (right). The shaded areas indicate the flat-top areas $\omega_{\mathrm{FT},i}$ of the respective PU functions arising from the scaling (2.3) with $\alpha = 1.25$. On level $k = 2$ we find one patch ω_i which overlaps the re-entrant corner and satisfies $\omega_i \cap \partial\Omega \neq \emptyset$ and $\omega_{\mathrm{FT},i} \cap \partial\Omega = \emptyset$. Thus, the respective PU function φ_i does *not* satisfy the flat-top condition on the boundary $\partial\Omega$.

The trace $\mathcal{B}_{D,n}(u^{\mathrm{PU}})$ of an arbitrary PPUM function

$$u^{\mathrm{PU}} = \sum_{i=1}^{N} \varphi_i \sum_{m=1}^{d_i} u_i^m \vartheta_i^m$$

obviously vanishes if the traces $\mathcal{B}_{D,n}(\vartheta_i^m)$ of *all* local approximation functions vanish, i.e.,

$$\mathcal{B}_{D,n}(u^{\mathrm{PU}}) = 0 \quad \Longleftarrow \quad \mathcal{B}_{D,n}(\vartheta_i^m) = 0 \quad \text{for all } (i,m) \tag{3.12}$$

with $i = 1, \ldots, N$, $m = 1, \ldots, d_i$ and $d_i = \dim(V_i)$. We obtain the equivalence

$$\mathcal{B}_{D,n}(u^{\mathrm{PU}}) = 0 \quad \Longleftrightarrow \quad \mathcal{B}_{D,n}(\vartheta_i^m) = 0 \quad \text{for all } (i,m) \tag{3.13}$$

if we assume that the employed PU satisfies a flat-top condition also for the Dirichlet boundary. For convex domains Ω this is automatically satisfied by our construction. However at re-entrant corners this boundary flat-top property is not ensured by the uniform isotropic scaling of (2.3), see Figure 2. Here, the introduction of a more general anisotropic scaling is necessary. The equivalence (3.13) yet is needed only to compute the (global) inverse of $B_{I,I}$ in (3.11). Fortunately, we can avoid the computation of the inverse of $B_{I,I}$ with respect to the global basis $\langle \varphi_i \vartheta_i^m \rangle$ in our PPUM. Thus our construction requires the implication (3.12) only and we can stick with the uniform isotropic scaling (2.3) in our cover construction also for non-convex domains Ω.

Let us consider a patch $\omega_i \cap \Gamma_{D,n} \neq \emptyset$ and its associated local approximation space $V_i(\omega_i) = \text{span}\langle \vartheta_i^m \rangle$ with $d_i = \dim(V_i)$. First, we discretize the trace operator $\mathcal{B}^{D,n}$ using the basis $\langle \vartheta_i^m \rangle$, i.e., we compute the (normal part of the) mass matrix $M_i^{D,n}$ on the Dirichlet boundary with the entries

$$(M_i^{D,n})_{k,l} = \int_{\Gamma_{D,n}} (\vartheta_i^k \cdot n)(\vartheta_i^l \cdot n)\ ds. \tag{3.14}$$

Then we compute the eigenvalue decomposition

$$O_i^T M_i^{D,n} O_i = D_i \quad \text{with } O_i, D_i \in \mathbb{R}^{d_i \times d_i} \tag{3.15}$$

of the matrix $M_i^{D,n}$ where

$$O_i^T O_i = \mathbb{I}_{d_i}, \quad (D_i)_{k,l} = 0 \quad \text{for all } k,l = 1,\dots,d_i \text{ and } k \neq l,$$

the transformation O_i^T is normal and D_i is diagonal. Let us assume that the eigenvalues $(D_i)_{k,k}$ are given in decreasing order, i.e. $(D_i)_{k,k} \geq (D_i)_{k+1,k+1}$. Then the matrices O_i^T and D_i are block-partitioned as

$$O_i^T = \begin{pmatrix} \tilde{O}_i^T \\ K_i^T \end{pmatrix}, \quad D_i = \begin{pmatrix} \tilde{D}_i & 0 \\ 0 & \kappa_i \end{pmatrix}$$

where the rows of the rectangular matrix K_i^T denote those eigenvectors of the discrete local trace operator $M_i^{D,n}$ that span the (numerical) kernel of $M_i^{D,n}$, i.e. the near-null space. The diagonal matrix κ collects the respective d_i^K vanishing (or small) eigenvalues of $M^{D,n}$, i.e. $(\kappa_i)_{k,k} < \epsilon\ (D_i)_{0,0}$. Hence the product operators

$$\Pi_{i,I}^{D,n} := \tilde{O}_i \tilde{O}_i^T = \begin{pmatrix} \mathbb{I}_{d_i^I} & 0 \\ 0 & 0 \end{pmatrix}, \quad \text{and} \quad \Pi_{i,K}^{D,n} := K_i K_i^T = \begin{pmatrix} 0 & 0 \\ 0 & \mathbb{I}_{d_i^K} \end{pmatrix}$$

with $d_i^I = d_i - d_i^K$ are the projections on the image of the discrete local trace operator $M_i^{D,n}$ and the kernel respectively. These projections operate on the new basis $\langle \tilde{\vartheta}_i^m \rangle$ given by the normal transformation

$$O_i^T : V_i = \operatorname{span}\langle \vartheta_i^m \rangle \to V_i = \operatorname{span}\langle \tilde{\vartheta}_i^m \rangle.$$

Furthermore, we obtain the local sub-spaces

$$V_{i,I} := \tilde{O}_i^T(V_i), \quad \text{and} \quad V_{i,K} := K_i(V_i).$$

Thus, the new basis $\langle \tilde{\vartheta}_i^m \rangle$ (i.e. the respective eigenfunctions of $\mathcal{B}^{D,n}$) provides a direct splitting

$$V_i = V_{i,K} \oplus V_{i,I}$$

of the local space V_i into a sub-space $V_{i,I}$ which is suitable for the approximation of the Dirichlet boundary conditions *locally* and a sub-space $V_{i,K}$ appropriate for the approximation of the PDE. Considering these local splittings for all $\omega_i \cap \Gamma_D \neq \emptyset$ (for the patches $\omega_i \cap \Gamma_D = \emptyset$ we set $V_{i,K} := V_i$) we obtain the corresponding direct splitting of the global PPUM space V^{PU}, i.e.

$$\sum_{i=1}^{N} \varphi_i V_i = V^{\mathrm{PU}} = V_K^{\mathrm{PU}} \oplus V_I^{\mathrm{PU}} := \sum_{i=1}^{N} \varphi_i V_{i,K} \oplus \sum_{i=1}^{N} \varphi_i V_{i,I} \tag{3.16}$$

and we obtain a partitioned global stiffness matrix A in the form (3.10) as the discretization of (3.1). Yet, the global discrete trace operator $B_{I,I}$ (which may not be invertible) of (3.10) was replaced by the block-diagonal operator $\hat{B}_{I,I} = (M_i^{D,n})$ that is by construction always invertible on the local sub-spaces $V_{i,I}$.

Note however that we do *not* need to assemble the stiffness matrix $A = A_{\tilde{\vartheta}}$ associated with the *classical* bilinear form (3.8) directly with respect to the computed basis $\langle \tilde{\vartheta}_i^m \rangle$ (which might require a fair amount of implementation). We can carry out the assembly of the stiffness matrix using the original basis $\langle \vartheta_i^m \rangle$ and apply the normal block-diagonal transformation T^T with the entries

$$(T^T)_{i,j} := \begin{cases} \mathbb{I}_{d_i} & j = i \text{ and } \omega_i \cap \Gamma_D = \emptyset, \\ O_i^T & j = i \text{ and } \omega_i \cap \Gamma_D \neq \emptyset, \\ 0 & j \neq i. \end{cases} \tag{3.17}$$

That is we attain the stiffness matrix $A_{\tilde{\vartheta}}$ in block-form (3.10) with respect to the new basis $\langle \tilde{\vartheta}_i^m \rangle$ as the triple-product[1]

$$A_{\tilde{\vartheta}} := T^T A_\vartheta T$$

via a simple post-processing operation. Furthermore, the blocks $A_{K,K}$ and $A_{K,I}$ given in (3.10) of $A_{\tilde{\vartheta}}$ can directly be computed with the help of the projections T_K^T and T_I^T where we just replace O_i^T in the definition (3.17) of T^T by K_i^T and $\tilde{O}_i^T$ respectively, i.e. we have

$$A_{K,K} := T_K^T A_\vartheta T_K, \quad \text{and} \quad A_{K,I} := T_K^T A_\vartheta T_I. \tag{3.18}$$

[1]Note however since T^T is block-diagonal this operation is easily parallelizable.

The matrix $B_{I,I}$ of (3.10) is replaced by the block-diagonal matrix $\hat{B}_{I,I}$. This matrix however is never explicitly formed and inverted. We rather implement the action of the inverse of $\hat{B}_{I,I}$ directly by local operations on the respective patches, see Step 7 in Algorithm 1.

Note that this purely algebraic approach which yields a conforming local treatment of essential boundary conditions also eliminates the first drawback of Nitsche's approach. The user may now interactively change the boundary conditions of (3.1). A change of the boundary configuration only affects the transformation T^T and thereby requires only local operations. There is no need to change the employed bilinear form; i.e., we do not need to derive a new weak form analytically nor do we need to compute a new regularization parameter β. There is also no need for a direct re-assembly of the stiffness matrix. We only need to update the respective block-entries of T^T in (3.17). The entries of T^T are computed from the local matrices $M^{D,n}$ which involve only the local approximation functions ϑ_i^m *not* the PU functions φ_i. Moreover, $M^{D,n}$ is an operator of order zero and defined on the Dirichlet boundary only. Hence, the computation of the respective integrals is much less involved than the direct assembly of the stiffness matrix for the product functions $\varphi_i\vartheta_i^m$ for patches ω_i overlapping the Dirichlet boundary.

Thus, a PPUM discretization of our model problem (3.1) using this conforming formulation of essential boundary conditions is summarized by the following algorithm.

Algorithm 1 (PPUM with automatic conforming boundary treatment).

1. Discretize the classical bilinear form (3.8) using the global basis $\langle\varphi_i\vartheta_i^m\rangle$ of the global space V^{PU} ignoring all boundary conditions. Denote the obtained global matrix A_ϑ.
2. Discretize the linear form
$$\langle l_\Omega, v\rangle := \int_\Omega fv \; dx$$
using the global basis $\langle\varphi_i\vartheta_i^m\rangle$ of the global space V^{PU} ignoring all boundary conditions. Denote the obtained global vector $\hat{f}_V$.
3. Discretize the linear form
$$\langle l_N, v\rangle := \int_{\Gamma_N} g_N v \; ds$$
associated with the Neumann boundary conditions using the global basis $\langle\varphi_i\vartheta_i^m\rangle$ of the global space V^{PU} for all patches $\omega_i \cap \Gamma_N \neq \emptyset$. Denote the obtained global vector $\hat{g}_N$.
4. Discretize the linear forms
$$\langle l^i_{D,n}, v\rangle := \int_{\omega_i\cap\Gamma_D} g_D(v\cdot n) \; ds$$

associated with the Dirichlet boundary conditions *locally* on each patch $\omega_i \cap \Gamma_D \neq \emptyset$ using the respective basis $\langle \vartheta_i^m \rangle$. Denote the obtained local vectors $\hat{g}_D^i$.

5. Discretize the bilinear forms

$$b_i(u,v) := \int_{\omega_i \cap \Gamma_D} (u \cdot n)(v \cdot n)\, ds$$

associated with the (restricted) trace operator *locally* on each patch $\omega_i \cap \Gamma_D \neq \emptyset$ using the respective basis $\langle \vartheta_i^m \rangle$. Denote the obtained local matrices $M_i^{D,n}$.

6. Compute the eigenvalue decompositions

$$O_i^T M_i^{D,n} O_i = D_i \quad \text{with } O_i, D_i \in \mathbb{R}^{d_i \times d_i}$$

of the local matrices $M_i^{D,n}$ on the respective patches $\omega_i \cap \Gamma_D \neq \emptyset$. Define the sub-matrices corresponding to the block-partitioning

$$O_i^T = \begin{pmatrix} \tilde{O}_i^T \\ K_i^T \end{pmatrix}, \quad D_i = \begin{pmatrix} \tilde{D}_i & 0 \\ 0 & \kappa_i \end{pmatrix}$$

by ordering the eigenvalues $(D_i)_{k,k}$ decreasingly such that $\tilde{D}_i$ is invertible.

7. Solve *locally* on each patch $\omega_i \cap \Gamma_D \neq \emptyset$ for the essential boundary conditions in $V_{i,I}$ via

$$\tilde{u}_{i,D} := \tilde{O}_i \tilde{D}_i^{-1} \tilde{O}_i^T \hat{g}_D^i.$$

Define the vector $\tilde{u}_I := (\tilde{u}_{i,D})$ which corresponds to a function $u_D \in V_I^{\mathrm{PU}}$ with $\mathcal{B}_{D,n}(u_D) = g_D$ on Γ_D.

8. Define the transformation T^T according to (3.17) and the respective projections $T_K^T : V^{\mathrm{PU}} \to V_K^{\mathrm{PU}}$ and $T_I^T : V^{\mathrm{PU}} \to V_I^{\mathrm{PU}}$. Define the blocks $A_{K,K}$ and $A_{K,I}$ according to (3.18).
9. Solve globally for the remaining degrees of freedom, i.e. solve in V_K^{PU}, via

$$\tilde{u}_K := A_{K,K}^{-1}(T_k^T(\hat{f}_V + \hat{g}_N) - A_{K,I}\tilde{u}_I). \tag{3.19}$$

10. Apply the transformation T^T to obtain the solution $\tilde{u}^{\mathrm{PU}}$ with respect to the original global basis $\langle \varphi_i \vartheta_i^m \rangle$ of the global space V^{PU}, i.e. set

$$\tilde{u}^{\mathrm{PU}} = T \begin{pmatrix} \tilde{u}_K \\ \tilde{u}_I \end{pmatrix}.$$

Note that the final representation of the solution $\tilde{u}^{\mathrm{PU}}$ is given with respect to the original basis $\langle \varphi_i \vartheta_i^m \rangle$ of the global PPUM space V^{PU} so that all implemented post-processing routines can be employed directly. There is no need for a change of the implementation.

Step 7 of Algorithm 1 corresponds to the solution of $B_{I,I}\tilde{u}_I = \hat{g}_D$ of (3.11). However the discrete global trace operator $B_{I,I}$ is replaced by the

block-diagonal matrix $\hat{B}_{I,I}$ of the discrete local trace operators $M_i^{D,n}$. The boundary value g_D is approximated with respect to the local bases $\langle \tilde{\vartheta}_i^M \rangle$ not the global basis $\langle \varphi_i \tilde{\vartheta}_i^M \rangle$.

Recall that the matrix $A_{K,K}$ is always invertible on V_K^{PU} due to the use of a flat-top PU. For the solution of (3.19) in Step 9 of Algorithm 1 we employ our multilevel solver [13,16,27] which employs specific local prolongation and restrictions operators. These transfer operators must also be transformed to the new basis, i.e., projected to V_K^{PU}.

3.1 Properties

Let us summarize some notable properties of the presented algebraic approach with allows for a conforming meshfree discretization scheme.

1. The only prerequisite of our approach is the use of a flat-top PU.
2. There is no assumption on the distribution of the particles $x_i \in P$ e.g. $P \cap \Gamma_D = \emptyset$ is acceptable.
3. There is no additional assumption on the local approximation space V_i employed in our PPUM construction due to our algebraic construction. The spaces V_i do *not* have to satisfy boundary conditions a priori. We automatically compute an appropriate splitting of the local approximation spaces V_i. Hence, the presented approach is directly applicable also to enriched PPUM approximations [28, 30]. Furthermore, we may even use enrichment functions to encode a complicated inhomogeneous boundary value easily with this approach.
4. The error bounds of [3] hold for the proposed PPUM scheme; i.e., we obtain an optimally convergent numerical method.
5. The proposed discretization scheme employs the classical weak formulation of the considered PDE only. Thus, there is no need for the analytical derivation of an appropriate weak form for the particular PDE. Hence, the incorporation of new PDE, i.e. new applications, in a PPUM implementation is substantially simplified. Furthermore, there is no need for the automatic computation of an appropriate regularization parameter as in Nitsche's method. The PPUM with conforming boundary treatment can be employed easily also in an explicit time-stepping scheme.
6. The configuration of boundary conditions can be changed efficiently by local operations only. There is no feedback into the weak formulation of the problem.
7. The global linear system that needs to be solved is of smaller dimension than with Nitsche's method.
8. The Dirichlet boundary data is approximated *locally* only, i.e. $B_{I,I}$ is replaced by the block-diagonal matrix $\hat{B}_{I,I}$ of the discrete local trace operators $M_i^{D,n}$. The blocks $M^{D,n}$ can be computed very efficiently since they involve only the local basis functions ϑ_i^m *not* the partition of unity

functions φ_i; i.e., we ignore the overlap of the patches in the approximation of the Dirichlet data. This corresponds to the construction of the localized L^2-projection employed in our multilevel solver [16, 27]. Due to this localization we can compute the splitting of the global space with (sub-)linear complexity $O(N^{\frac{d-1}{d}})$.

9. With respect to the new local basis $\langle \tilde{\vartheta}_i^m \rangle$ the blocks $M^{D,n}$ are diagonal, i.e., the operator $\hat{B}_{I,I}$ is diagonal with respect to the collection of the local bases $\langle \tilde{\vartheta}_i^m \rangle$.
10. If the geometry of a particular boundary segment $\omega_i \cap \Gamma_D$ is rather complicated or the employed local approximation space V_i on the respective patch ω_i is not rich enough to resolve the geometry of $\omega_i \cap \Gamma_D$, then the kernel of the discrete local trace operator will be empty. Thus all degrees of freedom of V_i are used for the approximation of the Dirichlet data and the PDE is considered on the patch ω_i only as a correction of the right-hand side via $A_{K,I}$.

4 Numerical Results

In this section we present some results of our numerical experiments using the proposed conforming PPUM discretization scheme discussed above. To this end, we introduce some shorthand notation for various norms of the error $u - u^{\mathrm{PU}}$, i.e., we define

$$e_{L^\infty} := \frac{\|u - u^{\mathrm{PU}}\|_{L^\infty}}{\|u\|_{L^\infty}}, e_{L^2} := \frac{\|u - u^{\mathrm{PU}}\|_{L^2}}{\|u\|_{L^2}}, e_{H^1} := \frac{\|u - u^{\mathrm{PU}}\|_{H^1}}{\|u\|_{H^1}}. \tag{4.1}$$

For each of these error norms we compute the respective algebraic convergence rate ρ by considering the error norms of two consecutive levels $l-1$ and l

$$\rho := -\frac{\log\left(\frac{\|u-u_l^{\mathrm{PU}}\|}{\|u-u_{l-1}^{\mathrm{PU}}\|}\right)}{\log(\frac{\mathsf{dof}_l}{\mathsf{dof}_{l-1}})}, \quad \text{where } \mathsf{dof}_q := \sum_{i=1}^{N_q} \dim(V_{i,q}). \tag{4.2}$$

Hence the optimal rate ρ_{H^1} of an uniformly h-refined sequence of spaces with $p_{i,k} = p$ for all $i = 1, \ldots, N_k$ and $k = 0, \ldots, J$ for a sufficiently regular solution u is $\rho_{H^1} = \frac{p}{d}$ where d denotes the spatial dimension of $\Omega \subset \mathbb{R}^d$. This corresponds to the classical $h^{\gamma_{H^1}}$ notation with $\gamma_{H^1} = \rho_{H^1} d = p$.

We consider the simple model problem

$$\begin{aligned} -\Delta u &= f \quad \text{in } \Omega \subset \mathbb{R}^d, \\ u &= g_D \quad \text{on } \Gamma_D \subset \partial\Omega, \\ \frac{\partial u}{\partial n} &= g_N \quad \text{on } \Gamma_N = \partial\Omega \setminus \Gamma_D, \end{aligned} \tag{4.3}$$

with different boundary configurations and a sequence of uniformly refined covers C_Ω^k with $\alpha = 1.3$ in (2.3) and local polynomial spaces $\mathcal{P}^{p_{i,k}} = \mathcal{P}^1$ on

all levels $k = 1, \ldots, J$ for the discretization of (4.3). The number of patches on level k is given by $N_k = 2^{dk}$ and the patch diameter by $\operatorname{diam}(\omega_{i,k}) =: 2h_k = 2^{-k}\alpha \operatorname{diam}(\Omega)$. Throughout this paper we employ $\epsilon = 10^{-12}$ in the construction of the direct local splittings.

To assess the properties of the presented algebraic treatment of essential boundary conditions in the PPUM we compare the obtained results with those of a PPUM discretization using Nitsche's approach. To this end, we consider two choices for the regularization parameter β in Nitsche's method: First, the optimal (smallest) regularization parameter estimated by (3.5) which yields $\beta_{\text{opt}} \approx 4h_k^{-1}$ and a very large regularization parameter $\beta_\infty = 10^6 h_k^{-1}$ on level k. Recall from Section 3 that we anticipate that the absolute values of the relative errors e obtained with the optimal parameter β_{opt} are smaller than those attained with the large regularization β_∞. Yet, the convergence rates ρ should not be affected by the variation of the regularization parameter.

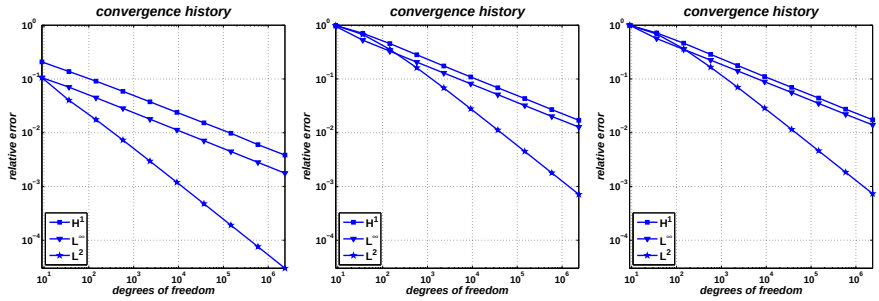

Fig. 3. Convergence history of the measured relative errors e (4.1) in the L^∞-norm, the L^2-norm, and the H^1-norm for Example 1 (left: Nitsche's method with β_{opt}, center: Nitsche's method with β_∞, right: algebraic conforming boundary treatment).

Example 1. In the first example we consider our model problem (4.3) on an L-shaped domain $\Omega = (-1, 1)^2 \setminus [0, 1]^2$. The Dirichlet boundary is given by

$$\Gamma_D := \{(x, y) \in \partial\Omega \,|\, x \geq 0 \text{ and } y \geq 0\}$$

the boundary segments which intersect at the re-entrant corner at $(0, 0)$. We choose $f = 0$, $g_D = 0$ and the Neumann boundary value g_N on $\Gamma_N = \partial\Omega \setminus \Gamma_D$ such that the analytic solution of (4.3) is given by the singular function

$$u(x, y) = u(r, \theta) = r^{\frac{2}{3}} \sin\left(\frac{2\theta - \pi}{3}\right) \tag{4.4}$$

where $r = r(x, y)$ and $\theta = \theta(x, y)$ denote polar coordinates; i.e., we consider homogeneous Dirichlet boundary data in this example.

In Table 1 we give the measured relative errors (4.1), the respective convergence rates (4.2) obtained with Nitsche's method using the optimal regularization β_{opt}. Furthermore, we give the number of levels J, the number of

Table 1. Relative errors e (4.1) and convergence rates ρ (4.2) using Nitsche's method with β_{opt} for Example 1.

J	dof	N	e_{L^∞}	ρ_{L^∞}	e_{L^2}	ρ_{L^2}	e_{H^1}	ρ_{H^1}
1	9	3	1.056_{-1}	–	1.060_{-1}	–	2.078_{-1}	–
2	36	12	7.051_{-2}	0.29	4.015_{-2}	0.70	1.379_{-1}	0.30
3	144	48	4.482_{-2}	0.33	1.753_{-2}	0.60	9.104_{-2}	0.30
4	576	192	2.833_{-2}	0.33	7.283_{-3}	0.63	5.890_{-2}	0.31
5	2304	768	1.787_{-2}	0.33	2.961_{-3}	0.65	3.764_{-2}	0.32
6	9216	3072	1.126_{-2}	0.33	1.191_{-3}	0.66	2.390_{-2}	0.33
7	36864	12288	7.095_{-3}	0.33	4.766_{-4}	0.66	1.527_{-2}	0.32
8	147456	49152	4.466_{-3}	0.33	1.900_{-4}	0.66	9.771_{-3}	0.32
9	589824	196608	2.809_{-3}	0.33	7.564_{-5}	0.66	5.996_{-3}	0.35
10	2359296	786432	1.764_{-3}	0.34	3.007_{-5}	0.67	3.832_{-3}	0.32

Table 2. Relative errors e (4.1) and convergence rates ρ (4.2) using Nitsche's method with β_∞ for Example 1.

J	dof	N	e_{L^∞}	ρ_{L^∞}	e_{L^2}	ρ_{L^2}	e_{H^1}	ρ_{H^1}
1	9	3	9.523_{-1}	–	9.884_{-1}	–	9.918_{-1}	–
2	36	12	5.273_{-1}	0.43	6.734_{-1}	0.28	7.078_{-1}	0.24
3	144	48	3.292_{-1}	0.34	3.567_{-1}	0.46	4.563_{-1}	0.32
4	576	192	2.060_{-1}	0.34	1.615_{-1}	0.57	2.821_{-1}	0.35
5	2304	768	1.293_{-1}	0.34	6.817_{-2}	0.62	1.746_{-1}	0.35
6	9216	3072	8.130_{-2}	0.33	2.787_{-2}	0.65	1.089_{-1}	0.34
7	36864	12288	5.121_{-2}	0.33	1.122_{-2}	0.66	6.854_{-2}	0.33
8	147456	49152	3.204_{-2}	0.34	4.490_{-3}	0.66	4.329_{-2}	0.33
9	589824	196608	2.014_{-2}	0.34	1.790_{-3}	0.66	2.695_{-2}	0.34
10	2359296	786432	1.276_{-2}	0.33	7.120_{-4}	0.66	1.707_{-2}	0.33

degrees of freedom dof, and the number of patches N. From these numbers we can clearly observe the anticipated optimal convergence behavior of Nitsche's approach with $\rho_{L^2} = \frac{2}{3}$ and $\rho_{H^1} = \frac{1}{3}$ for the approximation of a singular solution such as (4.4). On level $k = 10$ we attain the relative errors $e_{L^2} = 3.007_{-5}$ and $e_{H^1} = 3.832_{-3}$. The respective results using a large regularization β_∞ are given in Table 2. As expected the convergence rates ρ are not affected by the increase in the regularization parameter, again we find the optimal values $\rho_{L^2} = \frac{2}{3}$ and $\rho_{H^1} = \frac{1}{3}$. The absolute values of the relative errors however have increased by roughly one order of magnitude due to the larger regularization parameter, see also Figure 3. On level $k = 10$ we find $e_{L^2} = 7.120_{-4}$ and $e_{H^1} = 1.707_{-2}$. This growth of the absolute values of the relative error however can be regarded as the worst case since the error of the approximation (with β_{opt} and β_∞ respectively) attains its maximal value near the singularity of the solution which happens to be on the Dirichlet boundary.

The measured relative errors e and respective convergence rates ρ attained by the presented conforming approach are given in Table 3. Here, we give the number of degrees of freedom dof^I used to approximate the boundary conditions and the number of degrees of freedom $\mathsf{dof}^K = \mathsf{dof} - \mathsf{dof}^I$ used to approximate the PDE. Recall that our conforming approach corresponds to the limit case of Nitsche's method. Hence, we expect to find similar results as for β_∞. From the numbers displayed in 3 we can clearly observe this anticipated behavior. The convergence rates $\rho_{L^2} = \frac{2}{3}$ and $\rho_{H^1} = \frac{1}{3}$ are again

Table 3. Relative errors e (4.1) and convergence rates ρ (4.2) using the algebraic conforming boundary treatment for Example 1.

J	dof^K	dof^I	N	e_{L^∞}	ρ_{L^∞}	e_{L^2}	ρ_{L^2}	e_{H^1}	ρ_{H^1}
1	0	9	3	1.000_{0}	–	1.000_{0}	–	1.000_{0}	–
2	23	13	12	5.653_{-1}	0.41	6.872_{-1}	0.27	7.194_{-1}	0.24
3	123	21	48	3.561_{-1}	0.33	3.651_{-1}	0.46	4.645_{-1}	0.32
4	539	37	192	2.242_{-1}	0.33	1.657_{-1}	0.57	2.873_{-1}	0.35
5	2235	69	768	1.413_{-1}	0.33	7.000_{-2}	0.62	1.779_{-1}	0.35
6	9083	133	3072	8.891_{-2}	0.33	2.862_{-2}	0.65	1.109_{-1}	0.34
7	36603	261	12288	5.604_{-2}	0.33	1.153_{-2}	0.66	6.984_{-2}	0.33
8	146939	517	49152	3.507_{-2}	0.34	4.613_{-3}	0.66	4.412_{-2}	0.33
9	588795	1029	196608	2.204_{-2}	0.34	1.839_{-3}	0.66	2.745_{-2}	0.34
10	2357243	2053	786432	1.395_{-2}	0.33	7.315_{-4}	0.66	1.739_{-2}	0.33

optimal and the values of the relative errors on all levels correspond very well to those given in Table 2. On $k = 10$ for instance we find $e_{L^2} = 7.315_{-4}$ and $e_{H^1} = 1.739_{-2}$. The number of degrees of freedom used for the approximation of the Dirichlet boundary condition dof^I grows with $2^{d-1} = 2$. Note that on level $k = 1$ we have $\mathsf{dof}^K = 0$; i.e., on the coarsest level the PDE is not considered at all. The complete function space V^{PU} is used for the approximation of the Dirichlet boundary conditions and we obtain the approximate solution $u^{\mathrm{PU}} = 0$ due to $g_D = 0$, i.e., all relative errors are exactly 1.000_0. This is due to the fact that we use linear polynomials on each patch only; i.e., there are just three degrees of freedom associated with each local approximation space V_i. If a corner of the Dirichlet boundary is overlapped by a particular patch ω_i then all three degrees of freedom of V_i are required for the approximation of the linear traces on the boundary segment $\partial\Omega \cap \omega_i$, compare Figure 2. Hence, on *all* levels $k = 1, \ldots, J$ there are *no* internal degrees of freedom employed on patches ω_i that overlap the re-entrant corner at $(0, 0)$ or any other corner of Ω; i.e., near the corners of the domain Ω the PDE contributes to the approximation by a correction of the right-hand side only.

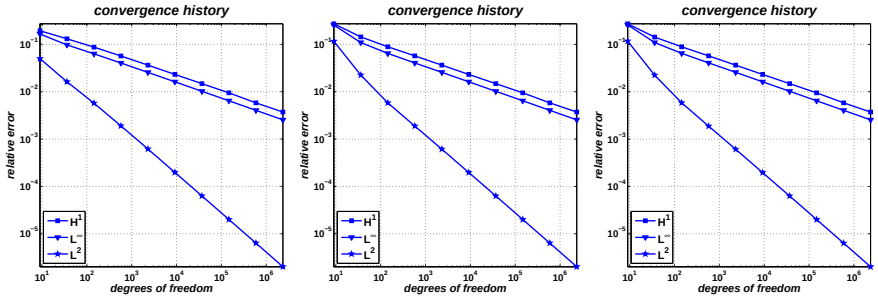

Fig. 4. Convergence history of the measured relative errors e (4.1) in the L^∞-norm, the L^2-norm, and the H^1-norm for Example 2 (left: Nitsche's method with β_{opt}, center: Nitsche's method with β_∞, right: algebraic conforming boundary treatment).

Table 4. Relative errors e (4.1) and convergence rates ρ (4.2) using Nitsche's method with β_{opt} for Example 2.

J	dof	N	e_{L^∞}	ρ_{L^∞}	e_{L^2}	ρ_{L^2}	e_{H^1}	ρ_{H^1}
1	9	3	1.657_{-1}	–	4.995_{-2}	–	1.937_{-1}	–
2	36	12	9.737_{-2}	0.38	1.623_{-2}	0.81	1.312_{-1}	0.28
3	144	48	6.325_{-2}	0.31	5.723_{-3}	0.75	8.733_{-2}	0.29
4	576	192	4.043_{-2}	0.32	1.900_{-3}	0.80	5.682_{-2}	0.31
5	2304	768	2.563_{-2}	0.33	6.157_{-4}	0.81	3.642_{-2}	0.32
6	9216	3072	1.619_{-2}	0.33	1.975_{-4}	0.82	2.316_{-2}	0.33
7	36864	12288	1.021_{-2}	0.33	6.304_{-5}	0.82	1.480_{-2}	0.32
8	147456	49152	6.430_{-3}	0.33	2.006_{-5}	0.83	9.466_{-3}	0.32
9	589824	196608	4.047_{-3}	0.33	6.363_{-6}	0.83	5.823_{-3}	0.35
10	2359296	786432	2.543_{-3}	0.33	2.017_{-6}	0.83	3.717_{-3}	0.32

Example 2. In our second example we consider (4.3) again on the L-shaped domain Ω. However now we choose the Dirichlet boundary Γ_D as

$$\Gamma_D := \{(x, y) \in \partial\Omega \,|\, x = -1 \text{ or } y = -1\}$$

and employ the data $f = 0$, and $g_D = u|_{\Gamma_D}$ and g_N such that (4.4) is again the analytic solution of (4.3); i.e., we consider inhomogeneous Dirichlet boundary data in this example. Observe that the Dirichlet boundary in this example is well-separated from the singularity of the solution at $(0, 0)$ where the maximal error occurs. Therefore, we expect to find a smaller increase in the measured relative errors due to the increase in the regularization parameter. For the optimal Nitsche method with β_{opt} we expect to find a similar quality of the approximation as in Example 1. We give the obtained results for β_{opt} in Table 4. Comparing these relative errors e_{H^1} with those of Table 1 clearly shows this asserted behavior. The numbers agree very well. For the relative errors e_{L^2} however we find a measurable improvement in this example. Instead of the expected convergence rate of $\rho_{L^2} = \frac{2}{3}$ we find $\rho_{L^2} \approx 0.8$. This is a pre-asymptotic effect due to the fact that the error is maximal *on* the Neumann boundary near the singular point $(0, 0)$.

The results attained with β_∞ are presented in Table 5. Since the Dirichlet boundary is well-separated from the maximal error we expect to find a close correspondence of these results to those of Table 4. This asserted behavior can be clearly observed from the given numbers and the plots depicted in Figure 4. The measured relative errors on all levels agree very well. Similarly, the numerical results obtained with the algebraic approach summarized in Table 6 are almost indistinguishable from those of Tables 4 and 5. This can also be observed from Figure 4.

These first two examples show that the quality of the approximation obtained with the proposed conforming boundary treatment corresponds very well with that of Nitsche's method for β_∞ as expected. In fact we obtain the same overall accuracy as the Nitsche method with optimal regularization β_{opt} if the pointwise error is small in the vicinity of the Dirichlet boundary.

Table 5. Relative errors e (4.1) and convergence rates ρ (4.2) using Nitsche's method with β_∞ for Example 2.

J	dof	N	e_{L^∞}	ρ_{L^∞}	e_{L^2}	ρ_{L^2}	e_{H^1}	ρ_{H^1}
1	9	3	2.553_{-1}	–	1.163_{-1}	–	2.721_{-1}	–
2	36	12	1.094_{-1}	0.61	2.244_{-2}	1.19	1.437_{-1}	0.46
3	144	48	6.437_{-2}	0.38	5.819_{-3}	0.97	8.891_{-2}	0.35
4	576	192	4.055_{-2}	0.33	1.885_{-3}	0.81	5.706_{-2}	0.32
5	2304	768	2.565_{-2}	0.33	6.132_{-4}	0.81	3.646_{-2}	0.32
6	9216	3072	1.619_{-2}	0.33	1.972_{-4}	0.82	2.316_{-2}	0.33
7	36864	12288	1.021_{-2}	0.33	6.300_{-5}	0.82	1.480_{-2}	0.32
8	147456	49152	6.430_{-3}	0.33	2.005_{-5}	0.83	9.467_{-3}	0.32
9	589824	196608	4.047_{-3}	0.33	6.362_{-6}	0.83	5.823_{-3}	0.35
10	2359296	786432	2.543_{-3}	0.33	2.017_{-6}	0.83	3.717_{-3}	0.32

Table 6. Relative errors e (4.1) and convergence rates ρ (4.2) using the algebraic conforming boundary treatment for Example 2.

J	dof^K	dof^I	N	e_{L^∞}	ρ_{L^∞}	e_{L^2}	ρ_{L^2}	e_{H^1}	ρ_{H^1}
1	2	7	3	2.573_{-1}	–	1.171_{-1}	–	2.718_{-1}	–
2	21	15	12	1.094_{-1}	0.62	2.241_{-2}	1.19	1.426_{-1}	0.47
3	113	31	48	6.450_{-2}	0.38	5.828_{-3}	0.97	8.878_{-2}	0.34
4	513	63	192	4.059_{-2}	0.33	1.875_{-3}	0.82	5.705_{-2}	0.32
5	2177	127	768	2.566_{-2}	0.33	6.093_{-4}	0.81	3.646_{-2}	0.32
6	8961	255	3072	1.619_{-2}	0.33	1.962_{-4}	0.82	2.316_{-2}	0.33
7	36353	511	12288	1.021_{-2}	0.33	6.276_{-5}	0.82	1.480_{-2}	0.32
8	146433	1023	49152	6.430_{-3}	0.33	2.000_{-5}	0.82	9.467_{-3}	0.32
9	587777	2047	196608	4.047_{-3}	0.33	6.350_{-6}	0.83	5.823_{-3}	0.35
10	2355201	4095	786432	2.543_{-3}	0.33	2.014_{-6}	0.83	3.717_{-3}	0.32

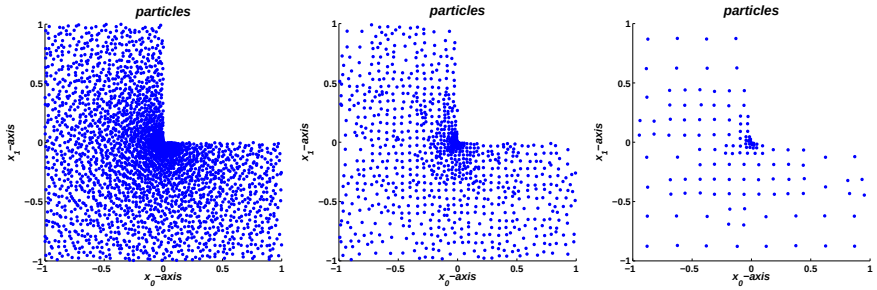

Fig. 5. Distribution of discretization points on level $k = 11$ (left), $k = 9$ (center), and $k = 7$ (right) employed in Example 3.

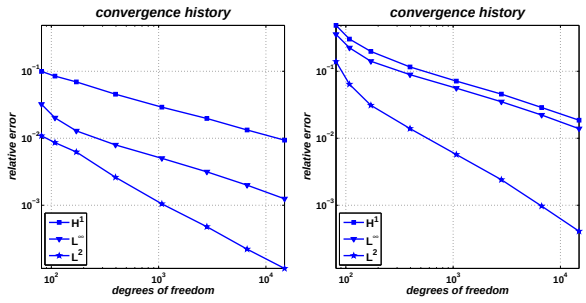

Fig. 6. Convergence history of the measured relative errors e (4.1) in the L^∞-norm, the L^2-norm, and the H^1-norm for Example 3 (left: Nitsche's method with β_{opt}, right: algebraic conforming boundary treatment).

Table 7. Relative errors e (4.1) and convergence rates ρ (4.2) using Nitsche's method with β_{opt} for Example 3.

J	dof	N	e_{L^∞}	ρ_{L^∞}	e_{L^2}	ρ_{L^2}	e_{H^1}	ρ_{H^1}
4	81	27	3.217_{-2}	–	1.087_{-2}	–	9.949_{-2}	–
5	108	36	2.018_{-2}	1.62	8.610_{-3}	0.81	8.482_{-2}	0.55
6	171	57	1.289_{-2}	0.98	6.231_{-3}	0.70	6.948_{-2}	0.43
7	396	132	7.956_{-3}	0.57	2.611_{-3}	1.04	4.550_{-2}	0.50
8	1071	357	5.013_{-3}	0.46	1.048_{-3}	0.92	2.912_{-2}	0.45
9	2817	939	3.153_{-3}	0.48	4.770_{-4}	0.81	1.976_{-2}	0.40
10	6678	2226	1.991_{-3}	0.53	2.209_{-4}	0.89	1.328_{-2}	0.46
11	14904	4968	1.247_{-3}	0.58	1.139_{-4}	0.82	9.364_{-3}	0.44

Table 8. Relative errors e (4.1) and convergence rates ρ (4.2) using the algebraic conforming boundary treatment for Example 3 using a graded particle set.

J	dof^K	dof^I	N	e_{L^∞}	ρ_{L^∞}	e_{L^2}	ρ_{L^2}	e_{H^1}	ρ_{H^1}
4	41	40	27	3.560_{-1}	–	1.394_{-1}	–	4.842_{-1}	–
5	64	44	36	2.242_{-1}	1.61	6.404_{-2}	2.70	3.028_{-1}	1.63
6	113	58	57	1.411_{-1}	1.01	3.103_{-2}	1.58	1.979_{-1}	0.93
7	306	90	132	8.897_{-2}	0.55	1.393_{-2}	0.95	1.160_{-1}	0.64
8	913	158	357	5.599_{-2}	0.47	5.711_{-3}	0.90	7.135_{-2}	0.49
9	2573	244	939	3.507_{-2}	0.48	2.406_{-3}	0.89	4.564_{-2}	0.46
10	6308	370	2226	2.223_{-2}	0.53	9.703_{-4}	1.05	2.877_{-2}	0.53
11	14358	546	4968	1.388_{-2}	0.59	4.092_{-4}	1.08	1.860_{-2}	0.54

Example 3. In our third example we focus on the robustness of our algebraic approach with respect to the distribution of the discretization points. Recall that our construction makes no assumption on this distribution. Thus the quality of the resulting conforming approach should correspond to that of Nitsche's approach independent of the positions of the employed discretization points. To confirm this assertion we discretize our model problem (4.3) on the L-shaped domain Ω with Dirichlet boundary $\Gamma_D = \partial\Omega$ using a graded Halton-point set, see Figure 5, for the construction of our cover sequence C^k_Ω. Again, we choose $f = 0$ and $g_D = u|_{\Gamma_D}$ to obtain the analytic solution (4.4). Due to the grading of the discretization points we should almost recover the convergence rates $\rho_{L^2} \approx 1$ and $\rho_{H^1} \approx \frac{1}{2}$ attainable for a regular solution.

In this example we only consider the optimal choice of β_{opt} in Nitsche's method and our algebraic approach. The attained relative errors and convergence rates are summarized in Tables 7 and 8 respectively. Both approaches yield the asserted approximation rates $\rho_{L^2} \approx 1$ and $\rho_{H^1} \approx \frac{1}{2}$. For the relative errors we find an increase by a factor of 4 (see also Figure 6). Hence, the constant in this example is slightly better than in Example 3.

and the achieved relative errors on all levels agree rather well, compare Figure 6.

Example 4. In our last example we consider the smooth solution

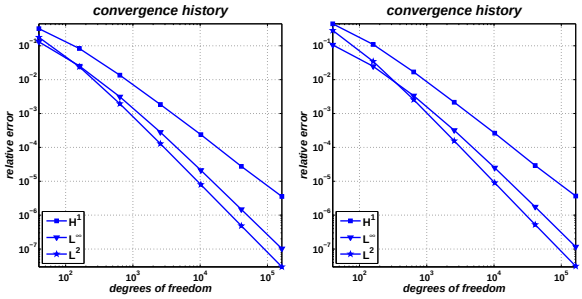

Fig. 7. Convergence history of the measured relative errors e (4.1) in the L^∞-norm, the L^2-norm, and the H^1-norm for Example 4 (left: Nitsche's method with β_{opt}, right: algebraic conforming boundary treatment).

Table 9. Relative errors e (4.1) and convergence rates ρ (4.2) using Nitsche's method with β_{opt} for Example 4.

J	dof	N	e_{L^∞}	ρ_{L^∞}	e_{L^2}	ρ_{L^2}	e_{H^1}	ρ_{H^1}
1	40	4	1.311_{-1}	–	1.777_{-1}	–	3.207_{-1}	–
2	160	16	2.536_{-2}	1.18	2.403_{-2}	1.44	8.312_{-2}	0.97
3	640	64	3.123_{-3}	1.51	1.944_{-3}	1.81	1.357_{-2}	1.31
4	2560	256	2.813_{-4}	1.74	1.283_{-4}	1.96	1.846_{-3}	1.44
5	10240	1024	2.114_{-5}	1.87	7.946_{-6}	2.01	2.382_{-4}	1.48
6	40960	4096	1.476_{-6}	1.92	4.851_{-7}	2.02	2.751_{-5}	1.56
7	163840	16384	1.020_{-7}	1.93	2.978_{-8}	2.01	3.555_{-6}	1.48

$$u(x,y) = \exp(4(x+y)) \tag{4.5}$$

of our model problem (4.3) for the sake of completeness on the domain $\Omega = (-1,1)^2$ with inhomogeneous Dirichlet boundary data $g_D = u|_{\Gamma_D}$. Here we employ a higher order PPUM approach with $p = 3$; i.e., we use cubic polynomials as local approximation spaces $V_i = \mathcal{P}^3$. Hence, the optimal rates attainable are $\rho_{L^2} = 2$ and $\rho_{H^1} = \frac{3}{2}$. The Dirichlet boundary in this example is given by

$$\Gamma_D := \{(x,y) \in [-1,1]^2 \,|\, x \in \{-1,1\}\}.$$

The results obtained with Nitsche's approach using the optimal regularization parameter β_{opt} are given in Table 9. From these numbers we can clearly observed the anticipated convergence behavior with $\rho_{L^2} = 2$ and $\rho_{H^1} = \frac{3}{2}$. On level $k = 7$ our PPUM approximation yields the relative errors $e_{L^2} = 2.978_{-8}$ and $e_{H^1} = 3.555_{-6}$. With our conforming algebraic boundary treatment we obtain the results given in Table 10. Again, we can observe an optimal convergence with the rates $\rho_{L^2} = 2$ and $\rho_{H^1} = \frac{3}{2}$. On level $k = 7$ our PPUM approximation yields the relative errors $e_{L^2} = 3.110_{-8}$ and $e_{H^1} = 3.672_{-6}$ which are of the same quality as those attained by Nitsche's method using an optimal regularization, compare Figure 7.

Table 10. Relative errors e (4.1) and convergence rates ρ (4.2) using the algebraic conforming boundary treatment for Example 4.

J	dof^K	dof^I	N	e_{L^∞}	ρ_{L^∞}	e_{L^2}	ρ_{L^2}	e_{H^1}	ρ_{H^1}
1	24	16	4	1.060_{-1}	–	2.838_{-1}	–	4.438_{-1}	–
2	128	32	16	2.470_{-2}	1.05	3.446_{-2}	1.52	1.093_{-1}	1.01
3	576	64	64	3.344_{-3}	1.44	2.561_{-3}	1.88	1.686_{-2}	1.35
4	2432	128	256	3.196_{-4}	1.69	1.559_{-4}	2.02	2.155_{-3}	1.48
5	9984	256	1024	2.501_{-5}	1.84	9.021_{-6}	2.06	2.632_{-4}	1.52
6	40448	512	4096	1.754_{-6}	1.92	5.237_{-7}	2.05	2.921_{-5}	1.59
7	162816	1024	16384	1.160_{-7}	1.96	3.110_{-8}	2.04	3.672_{-6}	1.50

5 Concluding Remarks

We presented an algebraic approach for the automatic construction of a direct splitting of a PPUM discretization space which allows for the conforming treatment of essential boundary conditions. The presented scheme is fully automatic and applicable to all PU-based methods provided that the employed PU satisfies the flat-top condition. There are no restrictions on the employed particle distribution nor on the employed local approximation spaces due to our construction. With the presented approach the implementation of essential boundary conditions in the meshfree PPUM is very simple and rather easy on the user: Every necessary operation is determined and completed automatically.

To our knowledge the PPUM with the proposed algebraic construction is the only meshfree or mesh-based method that allows for a conforming boundary treatment without any assumptions on the distribution of the discretization points or the employed basis functions.

Acknowledgement. This work was supported in part by the Sonderforschungsbereich 611 *Singular phenomena and scaling in mathematical models* funded by the *Deutsche Forschungsgemeinschaft*.

References

1. I. Babuška, U. Banerjee, and J. E. Osborn, *Meshless and Generalized Finite Element Methods: A Survey of Some Major Results*, in Meshfree Methods for Partial Differential Equations, M. Griebel and M. A. Schweitzer, eds., vol. 26 of Lecture Notes in Computational Science and Engineering, Springer, 2002, pp. 1–20.
2. ———, *Survey of Meshless and Generalized Finite Element Methods: A Unified Approach*, Acta Numerica, (2003), pp. 1–125.
3. I. Babuška and J. M. Melenk, *The Partition of Unity Method*, Int. J. Numer. Meth. Engrg., 40 (1997), pp. 727–758.
4. S. Beissel and T. Belytschko, *Nodal Integration of the Element-Free Galerkin Method*, Comput. Meth. Appl. Mech. Engrg., 139 (1996), pp. 49–74.
5. T. Belytschko and T. Black, *Elastic crack growth in finite elements with minimal remeshing*, Int. J. Numer. Meth. Engrg., 45 (1999), pp. 601–620.

6. T. Belytschko, N. Moës, S. Usui, and C. Parimi, *Arbitrary discontinuities in finite elements*, Int. J. Numer. Meth. Engrg., 50 (2001), pp. 993–1013.
7. J. S. Chen, C. T. Wu, S. Yoon, and Y. You, *A Stabilized Conforming Nodal Integration for Galerkin Mesh-free Methods*, Int. J. Numer. Meth. Engrg., 50 (2001), pp. 435–466.
8. J. Dolbow and T. Belytschko, *Numerical Integration of the Galerkin Weak Form in Meshfree Methods*, Comput. Mech., 23 (1999), pp. 219–230.
9. C. A. Duarte, L. G. Reno, and A. Simone, *A higher order generalized fem for through-the-thickness branched cracks*, Int. J. Numer. Meth. Engrg., 72 (2007), pp. 325–351.
10. C. A. M. Duarte, I. Babuška, and J. T. Oden, *Generalized Finite Element Methods for Three Dimensional Structural Mechanics Problems*, Comput. Struc., 77 (2000), pp. 215–232.
11. C. A. M. Duarte, O. N. H. T. J. Liszka, and W. W. Tworzydlo, *A generalized finite element method for the simulation of three-dimensional dynamic crack propagation*, Int. J. Numer. Meth. Engrg., 190 (2001), pp. 2227–2262.
12. C. A. M. Duarte and J. T. Oden, *hp Clouds – A Meshless Method to Solve Boundary Value Problems*, Numer. Meth. for PDE, 12 (1996), pp. 673–705.
13. M. Griebel, P. Oswald, and M. A. Schweitzer, *A Particle-Partition of Unity Method—Part VI: A p-robust Multilevel Solver*, in Meshfree Methods for Partial Differential Equations II, M. Griebel and M. A. Schweitzer, eds., vol. 43 of Lecture Notes in Computational Science and Engineering, Springer, 2005, pp. 71–92.
14. M. Griebel and M. A. Schweitzer, *A Particle-Partition of Unity Method for the Solution of Elliptic, Parabolic and Hyperbolic PDE*, SIAM J. Sci. Comput., 22 (2000), pp. 853–890.
15. ———, *A Particle-Partition of Unity Method—Part II: Efficient Cover Construction and Reliable Integration*, SIAM J. Sci. Comput., 23 (2002), pp. 1655–1682.
16. ———, *A Particle-Partition of Unity Method—Part III: A Multilevel Solver*, SIAM J. Sci. Comput., 24 (2002), pp. 377–409.
17. ———, *A Particle-Partition of Unity Method—Part V: Boundary Conditions*, in Geometric Analysis and Nonlinear Partial Differential Equations, S. Hildebrandt and H. Karcher, eds., Springer, 2002, pp. 517–540.
18. ———, *A Particle-Partition of Unity Method—Part VII: Adaptivity*, in Meshfree Methods for Partial Differential Equations III, M. Griebel and M. A. Schweitzer, eds., vol. 57 of Lecture Notes in Computational Science and Engineering, Springer, 2006, pp. 121–148.
19. F. C. Günther and W. K. Liu, *Implementation of Boundary Conditions for Meshless Methods*, Comput. Meth. Appl. Mech. Engrg., 163 (1998), pp. 205–230.
20. W. Han and X. Meng, *Some Studies of the Reproducing Kernel Particle Method*, in Meshfree Methods for Partial Differential Equations, M. Griebel and M. A. Schweitzer, eds., vol. 26 of Lecture Notes in Computational Science and Engineering, Springer, 2002, pp. 193–210.
21. A. Huerta, T. Belytschko, T. Fernández-Méndez, and T. Rabczuk, *Meshfree Methods*, vol. 1 of Encyclopedia of Computational Mechanics, Wiley, 2004, ch. 10, pp. 279–309.
22. Y. Krongauz and T. Belytschko, *Enforcement of Essential Boundary Conditions in Meshless Approximations using Finite Elements*, Comput. Meth. Appl. Mech. Engrg., 131 (1996), pp. 133–145.

23. Y. Y. Lu, T. Belytschko, and L. Gu, *A New Implementation of the Element Free Galerkin Method*, Comput. Math. Appl. Mech. Engrg., 113 (1994), pp. 397–414.
24. N. Moës, J. Dolbow, and T. Belytschko, *A finite element method for crack growth without remeshing*, Int. J. Numer. Meth. Engrg., 46 (1999), pp. 131–150.
25. J. Nitsche, *Über ein Variationsprinzip zur Lösung von Dirichlet-Problemen bei Verwendung von Teilräumen, die keinen Randbedingungen unterworfen sind*, Abh. Math. Sem. Univ. Hamburg, 36 (1970–1971), pp. 9–15.
26. M. A. Schweitzer, *Ein Partikel–Galerkin–Verfahren mit Ansatzfunktionen der Partition of Unity Method*, Diplomarbeit, Institut für Angewandte Mathematik, Universität Bonn, 1997.
27. ———, *A Parallel Multilevel Partition of Unity Method for Elliptic Partial Differential Equations*, vol. 29 of Lecture Notes in Computational Science and Engineering, Springer, 2003.
28. ———, *An adaptive hp-version of the multilevel particle–partition of unity method*, Comput. Meth. Appl. Mech. Engrg., (2008). accepted.
29. ———, *Hierarchical enrichment and local preconditioning in the particle–partition of unity method*, tech. rep., Sonderforschungsbereich 611, Rheinische Friedrich-Wilhelms-Univeristät Bonn, 2008. in preparation.
30. ———, *A particle-partition of unity method part viii: Hierarchical enrichment*, tech. rep., Sonderforschungsbereich 611, Rheinische Friedrich-Wilhelms-Univeristät Bonn, 2008. submitted.